

Influences of a small step on the side wall on detonation propagation

Yoko Seki, Tomoaki Honda, Wookyung Kim, Tomoyuki Johzaki, and Takuma Endo
Hiroshima University
Higashi-Hiroshima, Hiroshima, Japan

1 Introduction

The re-initiation phenomenon associated with the critical-tube-diameter problem of detonation studied to date is mostly such that the re-initiation occurs apart from the side wall of the extremely large space [1–3]. On one hand, another re-initiation phenomenon has been investigated, where a detonation wave initially propagating in a tube diffracts into another tube whose diameter is several times larger than that of the original tube. In this case, the re-initiation occurs near or on the side wall of the larger tube. It was found that the Mach reflection of the diffracted shock wave of the decaying detonation on the side wall plays an important role in the re-initiation phenomenon [4]. In connection with this issue, Ohyaï et al. [5] investigated the detonation diffraction and re-initiation using a channel of rectangular cross-section with a backward-facing step. The height and width of the step were 20 mm and 25 mm, respectively, and the ratio of the step height to the detonation cell width was varied from 3 to 13. They concluded that the distance between the position of re-initiation and the step increased with the cell width.

In the studies so far, the propagation of detonation has been investigated under the condition that the detonation wave propagated into the unconfined space or the space with a side wall where the height of the step h was larger than the detonation cell width λ ($h/\lambda \geq 3$). From the viewpoint of safety engineering in the actual gas transportation piping systems, however, it is important to clarify the characteristics of detonation propagation with respect to the small changes of the channel in the same order of magnitude as the detonation cell width. From the above, in the present study, we experimentally investigated the influences of disturbances on the propagation properties of a detonation using the backward-facing steps and the backward-facing slopes as well as the forward-facing steps and the forward-facing slopes, where the step height was in the same order of magnitude as the detonation cell width.

2 Experimental apparatus

Figure 1 shows the overview of the experimental arrangement. The experimental apparatus was composed of a small ignition sub-chamber, detonation tube, and test chamber. The total length and inner diameter of the experimental apparatus were 2650 mm and 100 mm, respectively. The small ignition sub-chamber was separated from the detonation tube by a Mylar film with a thickness of 150 μm . The

explosive gas mixture was ignited using a commercially available automobile spark plug (NGK, BKR5E), installed on the end-wall of the ignition sub-chamber. To promote the deflagration-to-detonation transition (DDT) in the detonation tube, we installed a Shchelkin spiral with a total length of 600 mm, a pitch of 50 mm, and a blockage ratio of 0.41. Moreover, we installed two piezoelectric-type pressure transducers to measure the detonation propagation speed.

In the test chamber, two smoked plates were installed to observe the cellular patterns depicted by the detonation wave. Figure 2(a) shows the two smoked plates installed in the test chamber. One was an aluminum alloy (A2017) plate with a length of 645 mm and a width of 98 mm, which was installed along the central axis of the test chamber (hereafter, this is called “the horizontal plate”). The leading edge of the horizontal plate against which the incident detonation impinged was shaped as a knife edge for minimizing the perturbation on the detonation. The other was a 2-mm-thick stainless-steel (SUS304) plate with a length of 640 mm perpendicular to the horizontal plate as shown in Fig. 2(a) (hereafter, this is called “the vertical plate”), whose width was so that the vertical plate was fitted to the test chamber as shown in Fig. 2(a).

We used four types of the horizontal plate: one with a forward-facing step, one with a backward-facing step, one with a forward-facing slope, and one with a backward-facing slope, as shown in Fig. 2(b). The height of the steps was 1, 2, or 5 mm, hereafter, positive values indicate the forward-facing steps and negative values indicate the backward-facing steps. In addition, the height of the forward-facing slopes and the backward-facing slopes was fixed to 5 mm, and the angles of the forward-facing slopes were 40° or 75° , while the angles of the backward-facing slopes were 20° or 40° . In the case of the forward-facing slopes, the slope angle of 40° corresponds to the Mach reflection of the leading shock wave, whereas the slope angle of 75° corresponds to the regular reflection of the leading shock wave.

In the present study, $2\text{H}_2+\text{O}_2+4.5\text{Ar}$ was used as the explosive gas mixture. The mixture was premixed using a circulation pump at initial pressure of 15–60 kPa and at room temperature. Although the detonation tube and the test chamber were filled with $2\text{H}_2+\text{O}_2+4.5\text{Ar}$, the ignition sub-chamber was filled with $2\text{H}_2+\text{O}_2$ at 120 kPa.

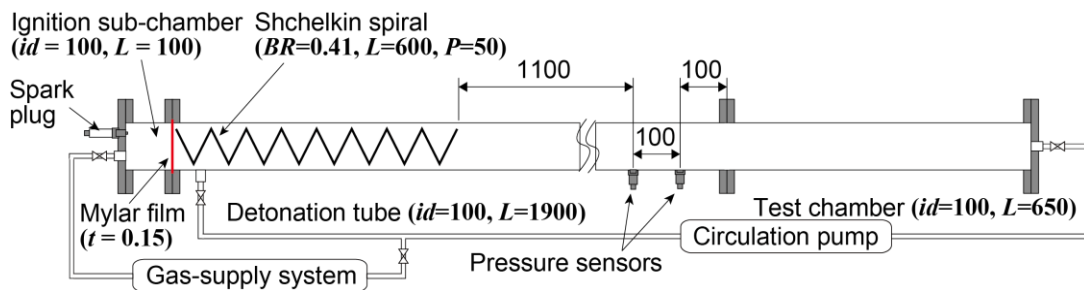


Fig. 1 Experimental arrangement (overview).

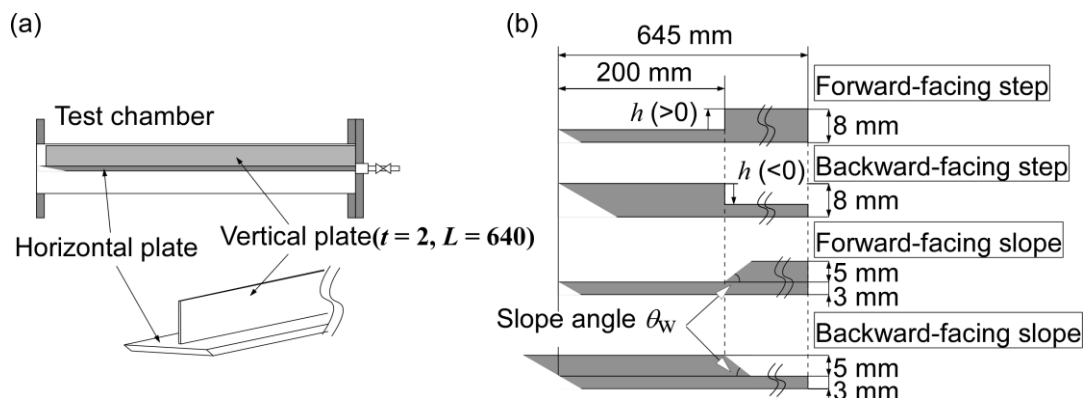


Fig. 2 (a) Two smoked plates in the test chamber. (b) Details of the horizontal plates.

3 Results and discussion

Figure 3 shows typical vertical and horizontal smoked-plate records obtained in the case of a forward-facing step. As shown in Fig. 3(a), a new transverse wave was created at the tip of the step. Such a new transverse wave was observed under all conditions of the forward-facing steps. On the other hand, the trajectories of the triple points seem to be continuous across the forward-facing step as shown in Fig. 3(b). Moreover, as shown in Fig. 3(a), no disturbance created by the forward-facing step was recognized in the cellular pattern except for the region quite near the tip of the step.

Figure 4 shows typical vertical and horizontal smoked-plate records obtained in the case of a forward-facing slope. As shown in Fig. 4(a), a new transverse wave was created at the end edge of the slope. Such a new transverse-wave was observed under all conditions of the forward-facing slopes. On the other hand, the trajectories of the triple points seem to be continuous across the forward-facing slope as shown in Fig. 4(b). Moreover, as shown in Fig. 4(a), no disturbance created by the forward-facing slope was recognized in the cellular pattern except for the region quite near the end edge of the slope.

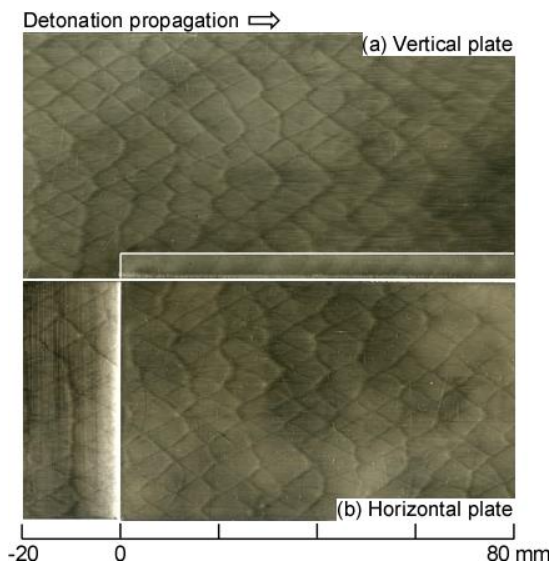


Fig. 3 (a) Vertical and (b) horizontal smoked-plate records obtained in the case of $h = +5$ mm and $p_0 = 30$ kPa .

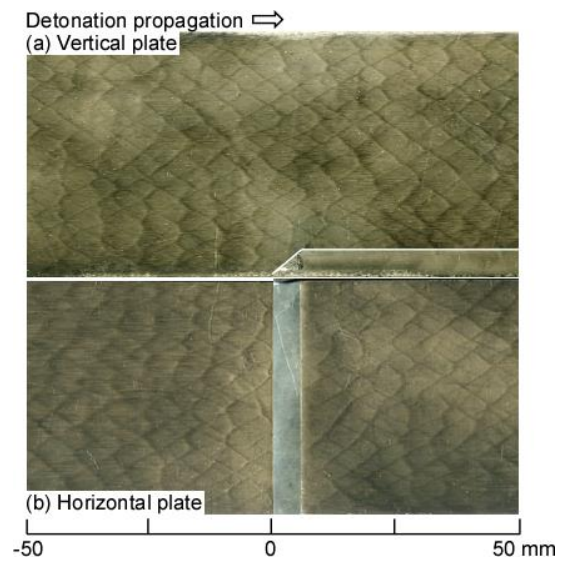


Fig. 4 (a) Vertical and (b) horizontal smoked-plate records obtained in the case of $\theta_w = 40^\circ$ and $p_0 = 30$ kPa .

In the case of the backward-facing step, the transverse-wave spacing became larger downstream of the step than those of the CJ detonation upstream of the step because of the rarefaction wave created by the backward-facing step. Furthermore, the re-initiation phenomenon occurred downstream of the step in some cases.

Figure 5 shows typical vertical and horizontal smoked-plate records obtained in the case of the backward-facing step. The calculated trajectory of the intersection of the head of the rarefaction wave and the leading shock wave [6,7] is depicted by the yellow dashed line originating from the tip of the step in Fig. 5(a). As shown in Fig. 5(a), in the upper region of the yellow dashed line, the cellular patterns were not affected by the rarefaction wave, while in the lower region, the cellular patterns were enlarged under the influence of the rarefaction wave. Moreover, traces of the re-initiation phenomenon are seen at the positions indicated by the yellow circles in Fig. 5(b). Furthermore, a strong transverse wave was generated at the position indicated by the arrow A in Fig. 5(a) and propagated toward the upper right direction. Behind the strong transverse wave, fine cellular patterns appeared on the vertical and horizontal smoked plates. That is, the re-initiation phenomenon occurred downstream of the step when $|h|/\lambda_{CJ} = 1.06$ where $h = -5$ mm and $\lambda_{CJ} = 4.72$ mm, and λ_{CJ} is the average value of the detonation cell

width measured at $x = -10$ mm (10 mm upstream the step) in each mixture condition. When the value of $|h|/\lambda_{CJ}$ was decreased to 0.56, fine cellular patterns were not recognized in the region downstream of the traces of the re-initiation phenomenon, where the re-initiation phenomenon was defined by the strong traces as shown by the yellow circles in Fig. 5(b). Summarizing the results, fine cellular patterns were recognized downstream of the traces of the re-initiation phenomenon only in the cases that the ratio $|h|/\lambda_{CJ}$ was more than unity approximately.

Figure 6 shows the detonation cell width λ observed in the cases of the backward-facing steps, where x denotes the position along the chamber axis relative to the position of the step and x_{ri} was the distance between the backward-facing step and the re-initiation position which was measured in the vertical smoked-plate. As mentioned above, fine cellular patterns were recognized only in the cases that $|h|/\lambda_{CJ}$ was more than unity approximately. As shown in Fig. 6, overdriven detonations were relaxed to CJ detonations propagating approximately ten times as long as the distance x_{ri} .

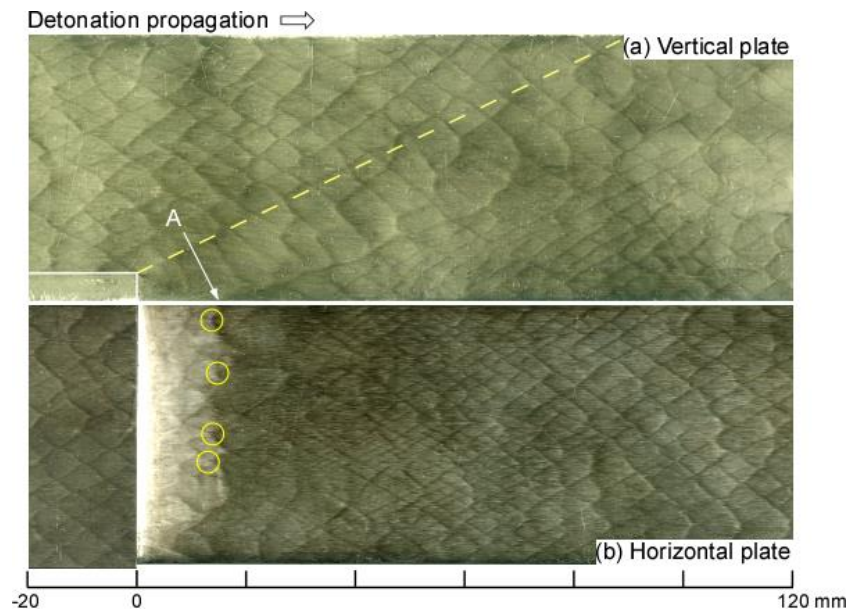


Fig. 5 (a) Vertical and (b) horizontal smoked-plate records obtained in the case of the backward-facing step of $|h|/\lambda_{CJ} = 1.06$.

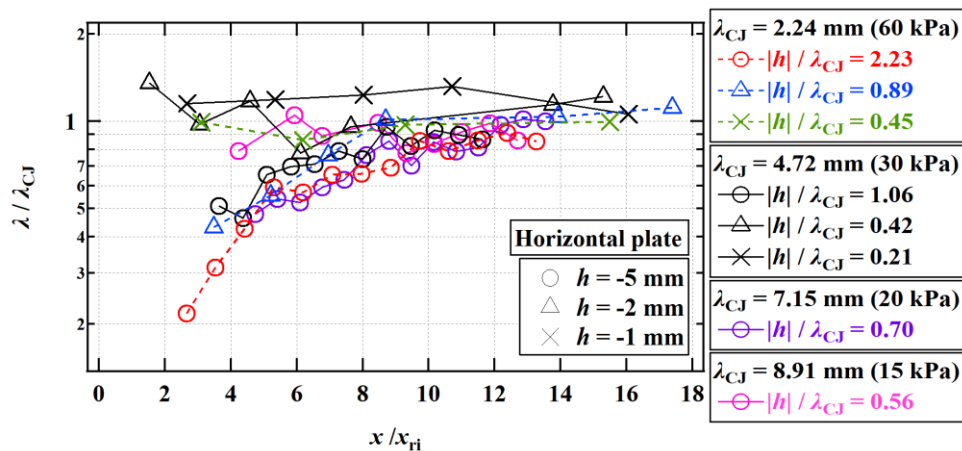


Fig. 6 Summary of the observed cell width λ downstream the backward-facing steps.

Figures 7 and 8 show typical vertical and horizontal smoked-plate records obtained in the cases of the backward-facing slopes of $\theta_w = 20^\circ$ and $\theta_w = 40^\circ$, respectively. As shown in Fig. 7, when $\theta_w = 20^\circ$, the cellular structure of the detonation did not disappear and the detonation continued to propagate on the backward-facing slope. As shown in Fig. 7, the cellular patterns were enlarged under the influence of the rarefaction wave over a distance of about 20 mm from the beginning of the slope ($x=0$). Subsequently, the cell width became smaller than λ_{CJ} once, and gradually relaxed to λ_{CJ} . This phenomenon is not understood well. When $\theta_w = 40^\circ$, traces of the re-initiation phenomenon are seen at the positions indicated by the yellow circles in Fig. 8(b) similarly to the case of the backward-facing

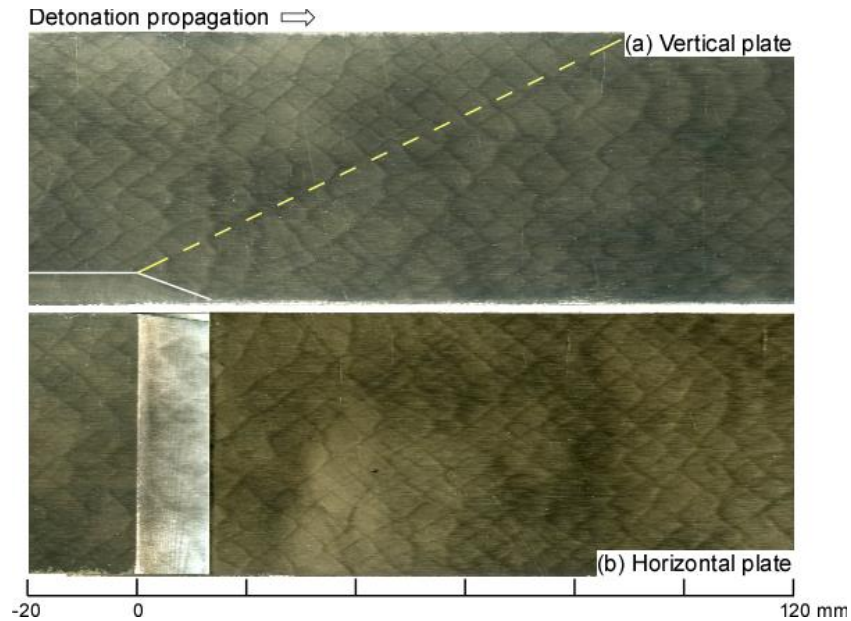


Fig. 7 (a) Vertical and (b) horizontal smoked-plate records obtained in the case of the backward-facing slope of $\theta_w = 20^\circ$ and $p_0 = 30$ kPa .

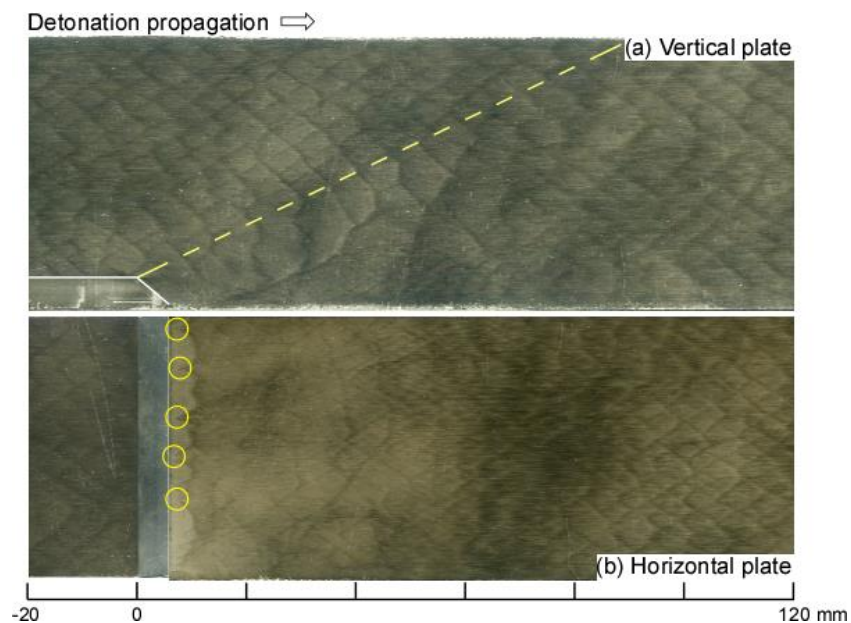


Fig. 8 (a) Vertical and (b) horizontal smoked-plate records obtained in the case of the backward-facing slope of $\theta_w = 40^\circ$ and $p_0 = 30$ kPa .

steps as shown in Fig. 5(b). Its difference from the backward-facing step is that the re-initiation phenomenon occurred just downstream the end of the slope. When the normal shock wave on the slope transits the boundary between the slope and the horizontal plate, the Mach reflection occurs on the horizontal plate. This may induce the re-initiation phenomenon. Moreover, the cellular pattern is similar to that of the backward-facing steps, namely the enlarged cellular patterns and the subsequent re-initiation phenomenon were observed.

4 Conclusions

We experimentally investigated the effects of a small obstacle on the side wall upon the detonation propagation. When the height of the forward-facing steps was the same order of magnitude as the cell width of the steady detonation λ_{CJ} , the effects of the steps were negligibly small. However, in the cases of the backward-facing steps, the cellular patterns were once enlarged under the influence of a rarefaction wave created by the backward-facing step, and subsequently the re-initiation phenomenon indicated by the strong traces downstream of the step on the smoked plate was observed and fine cellular patterns appeared downstream of the re-initiation position when the height of the step $|h|$ was larger than λ_{CJ} approximately. When the fine cellular patterns were recognized, overdriven detonations propagated approximately ten times as long as the distance between the backward-facing step and the re-initiation position x_{ri} . Moreover, in the case of the backward-facing slope with the slope angle $\theta_w = 40^\circ$, the enlarged cellular patterns and the subsequent re-initiation phenomenon were observed similarly to the cases of the backward-facing steps. However, in the case of the backward-facing slope with the slope angle $\theta_w = 20^\circ$, the cellular structure of the detonation did not disappear and the detonation continued to propagate.

Acknowledgments

This work was supported by JSPS KAKENHI Grant Number JP 20H02352.

References

- [1] Edwards DH, Thomas GO, Nettleton MA. (1979). The diffraction of a planar detonation wave at an abrupt area change. *J. Fluid Mech.* 95: 79.
- [2] Murray SB, Lee JHS. (1983). On the transformation of planar detonation to cylindrical detonation. *Combust. Flame* 52: 269.
- [3] Lee JHS. (1984). Dynamic parameters of gaseous detonations. *Annu. Rev. Fluid Mech.* 16: 311.
- [4] Pantow EG, Fischer M, Kratzel Th. (1996). Decoupling and recoupling of detonation waves associated with sudden expansion. *Shock Waves* 6: 131.
- [5] Ohyagi S, Obara T, Hoshi S, Cai P, Yoshihashi T. (2002). Diffraction and re-initiation of detonations behind a backward-facing step. *Shock Waves* 12: 221.
- [6] Pintgen F, Shepherd JE. (2009). Detonation diffraction in gases. *Combust. Flame* 156: 665.
- [7] Endo T, Kobayashi R, Kuwajima S, Seki Y, Kim W, Johzaki T. (2020). Detonation propagation from a cylindrical tube into a diverging cone. *J. Thermal Sci. Technol.* 15: 20-00283.